Ethiopian Journal of Science and Sustainable Development

e-ISSN 2663-3205 Volume 12 (1), 2025

Journal Home Page: www.ejssd.astu.edu.et

EJSSD
ETHIOPIAN JOURNAL OF SCIENCE AND SUSTAINABLE DEVELOPMENT

Research Paper

Drought vulnerability characterization and nature-based adaptation, Eerer Sub-Basin, Eastern Ethiopia

Asfaw Kebede[1,*], Dejene W. Sintayehu[2,3], Negash Tessema[4], Bekele Girma[4] and Jemal Yousuf[3]

[1]*Hydraulic and Water Resources Engineering Department, Haramaya University, Dire Dawa, P.O. Box 138, Ethiopia*
[2]*The Alliance of Biodiversity International and the International Center for Tropical Agriculture, Addis Ababa, P.O. Box 5689, Ethiopia*
[3]*College of Agriculture and Environmental Sciences, Haramaya University, Dire Dawa, P.O. Box 138, Ethiopia*
[4]*Water Resources and Irrigation Engineering Department, Haramaya University, Dire Dawa, P.O. Box 138, Ethiopia*

Article Info

Article History:
Received 22 September 2024
Received in revised form 09 December 2024
Accepted 14 December 2024

Keywords:
analytical hierarchy process,
climate change,
drought,
Eerer sub-basin,
GIS

Abstract

Over the past two decades, Ethiopia experienced recurrent and severe droughts, significantly impacting its environment, the livelihoods of its citizens, and the structure of its societal norms. To address these challenges, communities have increasingly turns to ecosystems as a natural buffer against the effects of climate change, particularly drought. The aim of this study was to analyze and to characterize drought-prone areas. The study highlighted the critical role of nature-based solutions (NbS) in climate change mitigation. Moreover, it proposed a long-term strategy to integrating NbS into disaster risk reduction plans by leveraging multi-sensor satellite data and other sources. The Analytical Hierarchy Process (AHP), Geographic Information System (GIS) and Remote Sensing (RS) were employed to evaluate drought vulnerability in the study area. The key variables considered for the study were elevation, slope, aspect, land uses and land cover, population density, normalized difference vegetation index, land surface temperature, normalized difference moisture index, vegetation condition index, vegetation health index, and soil moisture index. These metrics collectively provided a comprehensive assessment of drought conditions in the region. The findings revealed varying levels of drought severity: approximately 30.5 % of the study area is classified as experiencing medium drought, 19.1 % faces high drought, and 20 % shows no drought conditions. The results underscore the urgent need for a cohesive strategy to mitigate drought risks, focusing on climate adaptation and sustainable land management through NbS. This approach is vital for enhancing resilience and ensuring long-term sustainability in vulnerable regions.

1. Introduction

Climate change has exacerbated extreme weather conditions, such as excessive precipitation, extreme flooding, and hydro-meteorological droughts, in many parts of the world (Miralles, et al., 2019). The incidence and severity of hydrological and meteorological risks like wildfires, floods, cyclones, and sea level rise have risen due to climate change (Rather et al., 2022; Rehman et al., 2022; Mitchard, 2018). Particularly, the world is experiencing a critical time for continued rise in surface temperature; by the end of the century, temperatures are predicted to rise by up to 5°C (IPCC, 2021). However, with the imbalance in the natural elements brought on by climate change, weather occurrences become increasingly unpredictable. Over the past ten years,

*Corresponding author, e-mail: asfaw649@gmail.com

https://doi.org/10.20372/ejssdastu:v12.i1.2025.975

normal climatic phenomena have evolved into lethal threats that endanger humanity. There is an urgent need for water in many regions worldwide as the effects of climate change intensify. Although climate change impacts are felt globally, tropical countries are particularly vulnerable. Seasonal unpredictability, including prolonged summers and erratic monsoon arrivals and departures, have led to more floods and droughts.

The hydrological balance is affected by prolonged and abnormal dry weather conditions, which is referred to as a drought. Droughts are climatic disasters that occur on a global scale, with varying frequency and intensity (Baik et al., 2019; Rahmati et al., 2020). They have a significant impact on water availability as well as socioeconomic, and environmental activities (Deo et al., 2017). Hydrological droughts are characterized by a shortage of water in ponds, reservoirs, rivers, and aquifer, whereas meteorological droughts are caused by insufficient precipitation (Khoi et al., 2021). According to the drought special report of UNDRR (2021), at a temperature increase of 3 to 5°C, a severe to very severe drought will spread throughout central and eastern Ethiopia. In addition, droughts that afflicted roughly 1.5 billion people between 1998 and 2017 resulted in up to USD 124 billion in economic losses world-wide.

Additionally, human activities place immense stress on natural resources, leading to their overexploitation and degradation (Hasan & Rai, 2020). The increasing aridity in tropical river basins has been a focal point of research (Vu et al., 2017; Khatiwada & Pandey, 2019; Rehana & Naidu, 2021). For instance, Tadesse et al. (2017) reported that human interference has triggered a groundwater crisis and drought conditions in Ethiopia's Eerer Sub-basin. To better understand these challenges, researchers have emphasized the importance of assessing intensity, frequency, and occurrence of droughts using diverse variables (UNDRR, 2021). Innovative methodologies have been developed to address these issues. Ma et al. (2014) introduced an improved Standardized Palmer Drought Severity Index (SPDI) for precise spatiotemporal drought analysis worldwide. The Standardized Runoff Index (SRI) and Standardized Precipitation Index (SPI) were used by Vu et al. (2017) to evaluate hydrological and meteorological drought in Vietnam. Similarly, Sur et al. (2019) conducted a remote sensing-based assessment of agricultural drought using hydro-meteorological variables. In Kuwait, Alsumaiei & Alrashidi (2020) analyzed groundwater drought in desert areas using a condensed precipitation index. Various analytical approaches have also been employed to study drought, including examining its drivers, impacts, and responses (Lange et al., 2017). Khan et al. (2018) utilized neural network models, Lange et al. (2017) employed nonlinear autoregressive neural networks, and Azhdari et al. (2021) applied multivariate analysis and statistical methods for in-depth understanding of drought dynamics and the potential mitigation strategies.

The integration of Analytical Hierarchy Process (AHP) and Geographic Information System (GIS) has been extensively explored across various fields (Malczewski, 2006). For instance, Ying et al. (2007) developed an effective method combining AHP and GIS for regional eco-environmental evaluations. Similarly, multi-criteria assessment techniques integrated with GIS have yielded promising results in ecological modelling and managing flood and landslip hazards (Chen et al., 2011; Hasekiogullari & Ercanoglu, 2012; Stefanidis & Stathis, 2013; Demir et al., 2013). The integration of AHP and GIS was also applied in assessing drought risk. A notable example is the study conducted in Gubbi Taluk, Karna-taka, by Prakash et al. (2006). Their research was aimed to map drought severity using 17 GIS-based parameters influencing drought. The methodology involved developing a spatial database, assigning appropriate grading and ranking parameters, and integrating them into a GIS framework to create a drought intensity map. This approach demonstrated the potential of GIS and AHP in creating spatially robust drought assessments. Some other studies have also underscored the versatility and efficacy of integrating AHP with GIS for environmental and hazard assessments, including drought risk analysis (Palchaudhuri and Biswas, 2016; Ekrami et al., 2016; Sivakumar et al. 2021).

To ensure effective drought management, it is crucial to incorporate as many relevant parameters as possible across different categories of drought as feasible to derive comprehensive information on overall drought vulnerability. However, relatively few studies worldwide have successfully integrated multiple drought categories with sufficient criteria for assessing drought vulnerability. A recent study by Alharbi et al. (2022) examined drought vulnerability in the Kangsabati River Basin, Indian state of West Bengal, using an integrated approach that combined AHP and Geo-informatics. The research focused primarily on agricultural drought, employing various vulnerability factors to estimate drought risk. Despite its valuable insights, the study highlighted a broader gap in integrating multiple drought categories into vulnerability assessments. However, no study was conducted in Eerer sub-basin, which is vulnerable to drought, with comprehensive approach combining various drought categories with appropriate criteria.

Like other semiarid basins, Eerer Sub-basin has recently experienced significant hydro-meteorological hazards. To address these challenges, this research employed AHP to investigate the spatiotemporal distribution of drought-influencing factors across the region. Thus, the study aimed to analyze and characterize drought-vulnerable areas within the sub-basin, and it proposed a long-term solution by incorporating nature-based solutions (NbS) into disaster risk reduction plans. The findings provide scientific evidence for designing resilient and effective NbS that promote sustainability and benefit the society as well as the environment. Moreover, they have profound implications for the development and implementation of climate adaptation and biodiversity management policies.

2. Materials and Methods

2.1 Study area description

The study was conducted in Erer Sub-basin, which is part of the upper Wabi Shebelle Basin of Ethiopia, with elevation ranging from 800 to 2,920 m.a.s.l. (Dejene, et al., 2023). Geographically, the sub-basin is located between 08°12'35" and 09°31'07" N latitude and 42°04'27" and 42°31'07" E longitude (Figure 1).

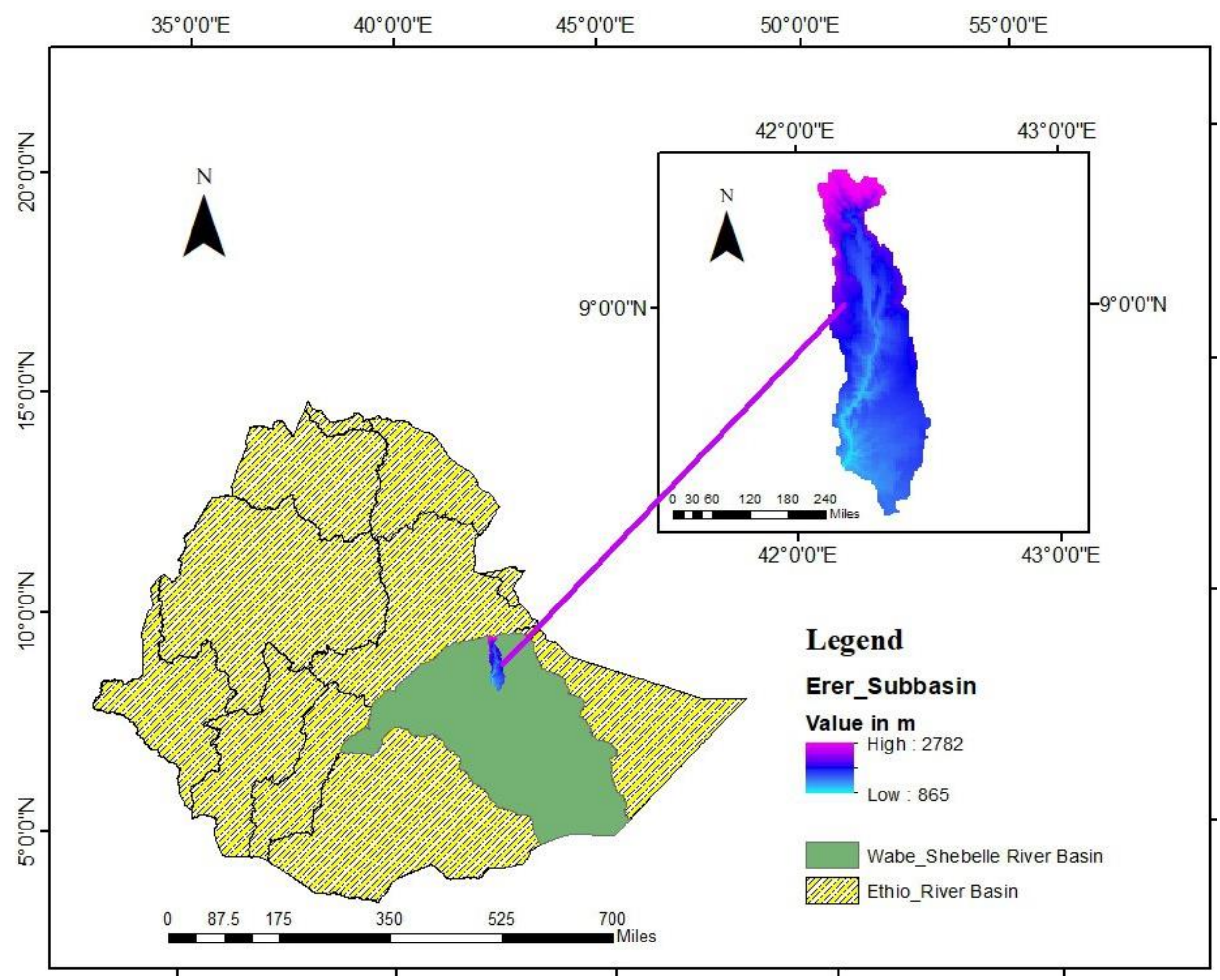

Figure 1: Location and elevation map of the study area

Covering a drainage area of 3,860 km^2, the sub-basin primarily falls within the 'kolla' climate classification (warm semiarid), which encompasses elevations between 500 and 1,500 m.a.s.l. and accounts for 73.5% of the area. According to Abrha (2016), the 'woina dega' climate (cool sub-humid; 1,500–2,300 m.a.s.l.) constitutes 25.12% of the area, while the 'dega' climate (cool humid; 2,300–3,200 m.a.s.l.) covers around 1.36%. Administratively, the sub-basin includes part of Harari Region and Kombolcha, Jarso, Babile, Midhagatola, and Fedis districts. The region experiences annual rainfall of 744 to 1017 mm, with most precipitation occurring during the summer months (MOA, 2000).

The average monthly maximum and minimum temperatures of the study area are 29.95 and 16.72 °C, respectively. The principal soil types are calcaric regosols (4%), eutric nitosols (8%), eutric regosols (20%), dystric cambisols (19%), haplic xerosols (33%), and humic cambisols (16%). These soil types collectively show diverse composition, influencing the area's agricultural and ecological characteristics.

2.2 Research design

To assess drought vulnerability, various factors were considered based on insights from previous studies. Thus, eleven drought indicators were selected to analyze drought occurrence in the study area by integrating GIS, Remote Sensing, and AHP. The indicators include elevation, slope, aspect, land use and land cover (LULC), population density, normalized difference vegetation index (NDVI), land surface temperature (LST), normalized difference moisture index (NDMI), vegetation condition index (VCI), vegetation health index (VHI), and soil moisture index (SMI). AHP was employed to assign relative weights of influence to each criterion, drawing on expert opinions rather than assuming equal weights for all parameters (Hasekiogullari & Ercanoglu, 2012). A weighted overlay analysis was then applied to standardize the data and to integrate the weights into thematic maps (Feizizadeh & Blaschke, 2013). After generating a drought vulnerability map, a prospective drought risk management strategy was developed using input collected from stakeholders during focus group discussion (FGD). The study also utilized Living Labs approach (Atteslander, 2003), to enable participatory planning and interactive processes for drought risk reduction. This approach, rooted in NbS, is crucial for incorporating stakeholders' perspectives and fostering effective drought mitigation strategies. The comprehensive methodology used is illustrated in Figure 2.

2.3 Datasets and standardization

To meet the research objectives, data was collected and organized from both primary and secondary sources. FGDs were conducted in the sub-basin, which was divided into two groups. Each of the five districts included in the Sub-basin had its own separate FGD. Each discussion involved between seven and twelve participants. The focus of the discussion was on the fluctuations of drought, over the past 30 years. Participants who were over the age of 30 were intentionally selected, as it was believed that their experiences would provide valuable insights into the drought conditions of the past three decades.

Furthermore, GPS data was utilized to identify areas vulnerable to drought. Population density data for all regions at district level, from 2014 – 2017, was obtained from the Central Statistical Agency (CSA) of Ethiopia (CSA, 2013), and summarized (Table 1). Additionally, Senti-nel-2A imagery from 2014 to 2020 was used to create LULC maps, as along with maps for NDVI, LST, NDMI, VCI, VHI, and SMI. These maps ensured cloud-free coverage at a resolution of 10×10 m. Satellite data from LANDSAT8 (OLiTRS) was also incorporated for analysis. Furthermore, the Alaska Digital Elevation Model (DEM) data, with a resolution of 12.5 ×12.5 m, was utilized for watershed delineation and to analyze elevation, slope, and aspect.

During the data analysis phases, various methods were employed to ensure the accurate selection, organization, processing, editing, clearing, and verification of input criteria. Field validation, validating digitization, data integration, and transformation were also conducted to locate pertinent information, to provide recommendations, and to support decision-making. Thematic layers were converted into a raster data format following standardization guidelines, and these layers were subsequently classified using insights from extensive literature review and expert knowledge.

Key vegetation and environmental indices were calculated by using equations 1 to 3, given by Myneni, et al. (1995), Jackson,et al. (2004) and Kogan (1997), respectively.

$$NDVI = \frac{NIR-RED}{NIR+RED} \quad (1)$$

$$NDMI = \frac{NIR-Green}{NIR+Green} \quad (2)$$

$$VCI = (NDVI - NDVI_{min}) / (NDVI_{max} - NDVI_{min}) \quad (3)$$

where NDVI is Normalized Difference Vegetation Index, NDMI is Normalized Difference Moisture Index, and VCI is Vegetation Condition Index.

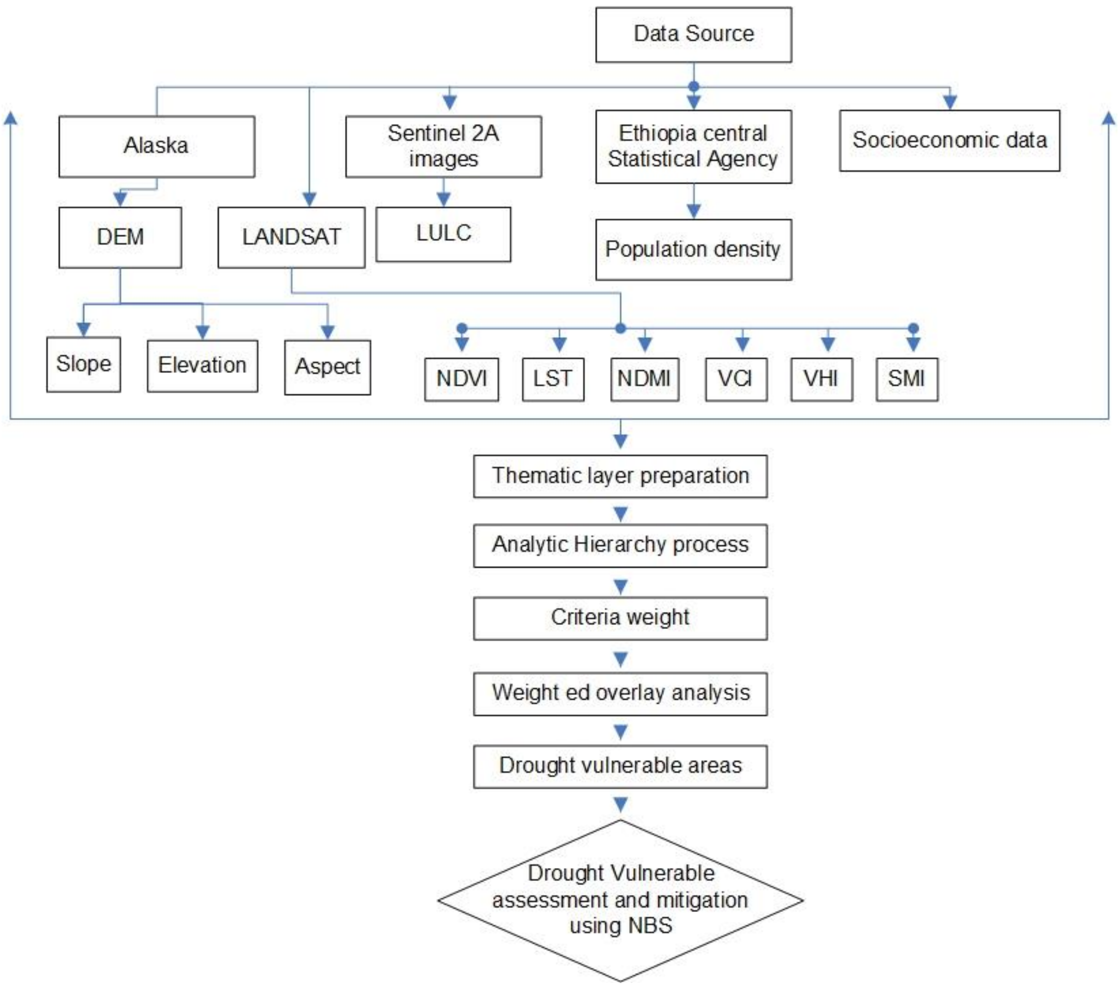

Figure 2: Overall Methodology (framework) used for drought vulnerability study of Eerer Sub-basin

Table 1: Sources of data

Data set	Year	Scale	Data type	Data source
Satellite image	2015, 2016, 2018, 2020	10×10m	Raster format	http://earthexplorer.usgs.gov/
DEM		12.5×12.5m	Raster format	https://www.asf.alaska.edu
GPS	2022	Point measurement	Different LULC classes & drought vulnerable areas	Field Survey
Population	Projected (2014 – 2017)	-	Number	CSA., 2013

To calculate Land surface temperature (LTS), the following intermediate steps, were performed (Valor & Caselles, 1996; Artis & Carnahan, 1982; Chander et al., 2009):

1. Digital Numbers (DN) were converted to spectral radiance using:

   $$Lk = ML \times QCAL + AL \tag{4}$$

   where ML and AL are sensor-specific calibration coefficients
2. Spectral radiance was transformed into brightness temperature (TB) in degree Celsius:

   $$TB = \frac{K2}{ln\left(\frac{K1}{L_k}+1\right)} - 273.15 \tag{5}$$

3. Proportion of Vegetation (PV) was estimated as:

   $$PV = \left[\frac{NDVI-NDVI_{min}}{NDVI_{max}-NDVI_{min}}\right]^2 \tag{6}$$

4. Land Surface Emissivity was estimated using:

   $$LSE = 0.004 \times PV + 0.986 \tag{7}$$

5. Finally LST was computed as:

   $$LST = \frac{BT}{1+W\times\left(\frac{BT}{14380}\right)\ln(E)} \tag{8}$$

   Additionally, VHI, a combined indicator of moisture and temperature, was calculated as:

   $$VHI = a*VCI + (1- a)*TCI \tag{9}$$

   where '*a*' is a coefficient that determines the relative contributions of each index (Kogan, 1997).

2.4 AHP and GIS model

A pairwise comparision matrix of relevant variables was created, and the AHP methods were then incorporated into GIS model. In AHP, the hierarchy is ordered with the overarching objective at the top, and the criteria, sub-criteria, and choices are listed in decreasing order. The user uses a comparison matrix at each level, comparing pairs of criteria to employ the comparative judgment principle. Using a scale of 1 (in difference) to 9 (strong preference), the parameters are compared pairwise (Table 2). Once the matrix of pairwise contrasts has been built using a comparative scale proposed by Saaty (2008), it is possible to evaluate the relative importance of each of the possibilities in terms of the specific standard. A composite weight was assigned to each alternative based on preferences established by a matrix of criteria or sub-criteria. Typically, the choice that was ultimately selected is the one that garnered the highest overall rating.

The importance of each criterion in evaluating drought threats was carefully considered in determining the weightings to be applied to each drought related factors.The eigenvector method was employed to calculate weights, with the largest eigenvalue serving as a critical component of this process.The primary input for determining the weightings was the pairwise comparison matrix of *n* criteria, constructed using Saaty's significance scale (Table 2).

Table 2: Intensity of Importance scale as suggested by (Saaty, 2008)

Intensity of importance	Definition	Explanation
1	Parameters are of equal importance	Two parameters contribute equally to the objective
3	The parameter I is of more importance compared to parameter J	Experience and judgment strongly favor I over J
5	Essential or strong importance of I compared to J	Experience and judgment strongly favor I over J
7	Very strong or demonstrated importance	Criteria I is very strongly favoured over J and its dominance is demonstrated in practice
9	Absolute importance	The evidence favoring, I over J to the highest possible order of affirmation
2,4,6,8	Intermediate values between two adjacent judgments	Judgment is not precise enough to assign values of 1, 3, 5, 7, and 9 (compromise is needed)

As demonstrated by Ahamed et al. (2000), the matrix typically takes the form of (n * n), where each entry represents the relative importance of a criterion compared to another:

$$A = [a_{ij}]; i, j = 1, 2, 3, \ldots, n \quad (10)$$

where $a_{ij} = \frac{w_i}{w_j}$ $for\ all\ i\ and\ j$ (11)

The matrix A generally has the property of reciprocity and also consistency. Mathematically,

$a_{ij} = 1/a_{ji}$, and $a^{ij} = a_{ik}/a_{jk}$ for any i, j and k.

Thus, multiplying Eq. (10) with the weighting factor W of (n * 1) size yields:

$$(A - nI) \times W = 0 \quad (12)$$

As a judgement matrix, A's components may not be able to be identified with sufficient precision to meet the consistency required. As a result, it may be calculated using a set of homogeneous linear equations: where *I* is the identity matrix of (n * n). Based on matrix theory, the system of equations has a simple solution if the comparison matrix A possesses attribute of consistency.

$$A^* \times W^* = \lambda max\ W^* \quad (13)$$

where *W** is the associated priority vector, *A** is the estimate of *A*, and *λmax* is the greatest eigenvalue for matrix A. The weightages W, which are normalized to unity, are produced by equation (13).

Where elements are equal to 1, the value of each unit is compared using an eleven by eleven pairwise reference matrix of diagonals (Table 3). The other values in each row indicate the relative importance of variables compared to one another. A pairwise evaluation matrix, a relative weight matrix, and a normalized principal Eigenvector were used to rank each parameter. To estimate the normalized principal eigenvector, the total of the column's values was divided by the corresponding relative weight matrix. Subsequently, normalized principal eigenvector was created by averaging the values in each row. Using this eigenvector, the percentages outcomes for each thematic layer were then determined.

The valuation of the consistency through pairwise evaluations is to assign the Consistency Ratio, CR (Al-Shabeeb et al., 2016). This step involves:

Step 1: Establishing decision hierarchy

A prioritization technique was used to rank the factors according to their relevance in making the decision at each level of the hierarchy once the hierarchy had been established (Saaty, 2008). Analytical hierarchy structure of areas vulnerable to drought. To better comprehend decision to be made, standard to be applied, and alternatives to be assessed, important to decompose a structure hierarchically (Demisachew et al. 2022).

Table 3: Matrix of pairwise comparisons between the chosen parameters

Parameters	NDVI	VCI	LST	LULC	VHI	SMI	NDMI	Slope	Population density	DEM	Aspect
NDVI	1	2	2	2	3	4	5	7	8	8	9
VCI	0.50	1	2	3	3	4	5	6	7	8	9
LST	0.50	0.50	1	2	3	3	3	5	6	7	8
LULC	0.50	0.33	0.50	1	2	3	3	4	4	5	7
VHI	0.33	0.33	0.33	0.50	1	1	2	4	5	6	7
SMI	0.25	0.25	0.33	0.33	1.00	1	1	2	3	5	5
NDMI	0.20	0.20	0.33	0.33	0.50	1.00	1	3	5	5	6
Slope	0.14	0.17	0.20	0.25	0.25	0.50	0.33	1	2	3	3
Population density	0.13	0.14	0.17	0.25	0.20	0.33	0.20	0.50	1	3	4
DEM	0.13	0.13	0.14	0.20	0.17	0.20	0.20	0.33	0.33	1	1
Aspect	0.11	0.11	0.13	0.14	0.14	0.20	0.17	0.33	0.25	1	1
Total	3.79	5.16	7.13	10.01	14.26	18.23	20.90	33.17	41.58	52.00	60.00

Step 2: Computing the consistency index (CI)

$$CI = \frac{\lambda_{max} - n}{n - 1} \quad (14)$$

where n is the number of components in the pair-wise comparison matrix and λmax is its Eigen value.

Step 3: Calculating CR

$$CR = \frac{CI}{RI} \quad (15)$$

where RI is the reciprocal matrix's consistency index, which was generated at random using the forced reciprocals on a scale of 1 to 9 (Table 4). A similar-sized pair-wise comparison matrix that was generated at random has an average consistency index.

Table 4: Random index for consistency/ inconsistency check (RI) (Source: Saaty, 2008)

N	1	2	3	4	5
R₁	0.00	0.00	0.58	0.90	1.12
N	6	7	8	9	
R₁	1.24	1.32	1.41	1.40	

Step 4: Defining the relative weight

The AHP method uses the CR, which should be less than or equal to 10%, to evaluate the consistency of the expert judgements (Al-Shabeeb et al., 2016). All the indicated parameters have CR of less than 10%. Hence, all parameters are used as an aggregation for computing the weights of each parameter.

Then, to efficiently identify potential drought hazard locations, a weighted overlay analysis was used. The eleven environmental factor maps were employed to create a zonation map of drought risk for the research area. These factors were numerically rated on a scale from 1 to 5, reflecting their relative importance. Weights and ranks were assigned to the class within the factors, with higher values indicating a greater impact on drought likelihood. Using the weighted overlay technique in GIS, the factors were integrated as thematic layers to produce the drought hazard zone map. The drought map was created after multiplying all the parameters by their respective weights (eqn. 16). The resulting drought map categorized the area into five zones of very high, high, medium, low and no drought.

$$D = \sum_{i=1}^{n} T_i * d_i \quad (16)$$

where *Ti* stands for each parameter's weights times the drought parameters (di).

2.5 Stakeholder perspectives on drought vulnerable areas using NbS

A qualitative approach was adopted to examine the stakeholders' perspectives on drought prone areas using NbS, participatory procedures, and collaborative planning techniques, utilizing a Living Labs approach (Atteslander, 2003). Living Labs serve as open innovation ecosystem centered on user through co-creation, integrating research and innovation in real life settings. By focusing on people, living labs adapt innovative concepts to local contexts, cultures, and aspirations, fascinating the co-creation of tailored solutions.

To collect in-depth qualitative data, this study employed FGD with a small, diverse group of participants (Marshall & Rossman, 1998). A systematic stakeholder mapping methodology (Zingraff-Hamed, et al., 2020) was used to identify potential participants based on available documents, local protocols, and site-specific information. Stakeholder selection followed the principle of maximum contrasts, depending on ground theory (Strauss & Corbin, 1990), to address diverse perspectives, attitudes, and opinions. Criteria for inclusion encompassed socio-demographic diversity, professional backgrounds, and viewpoints. Stakeholders were categorized into groups based on collected data, with adjustments made during the process to replace non-responsive or less relevant participants (Strout, et al., 2021).

Local facilitators' teams managed stakeholder processes, evaluating roles across co-design, co-implementation, and co-monitoring/evaluation phases. Using interest-influence matrices and three-dimensional power-influence-attitude grids (Reed, et al., 2009; Dejene et al., 2023), facilitators analyzed stakeholder interrelations and their susceptibility to drought risks. Additional considerations included stakeholders' potential contributions to NbS and their involvement in decision-making for identifying viable drought risk mitigation strategies.

Moreover, based on the results of the stakeholder mapping, participants at the various sites around the sub-basin were selected for FGD in iterative approach.

The FGD panel included at least one person from each of the following fields: industry, academia, politics, the government, and civil society (represented, for instance, by local NGOs). Murray-Webster & Simon (2006) deemed that the respondents' backgrounds and socio-demographic characteristics across all case locations should encompass a wide variety of perspectives, varied views, opinions, and backgrounds. However, in this study, not all of the individuals who were initially selected could be questioned because some declined the invitation to FGD or said they could not participate at the scheduled time. Thus, they were replaced. Phone and video conversations were also used for the FGDs. When FGD participants declined to be recorded, notes were taken. For the evaluation, audio recordings of FGDs were transcribed and interpreted into English from the local language, both Amharic and Afaan Oromo. The texts were then evaluated, condensed, and organized under or into essential assertions and relative frequency (Hunziker, 2000).

Spatial planning and management strategies must consider the potential of NbS to mitigate drought in valuable areas and provide sustainable solutions (Mayring, 2010). Thus, following the development of the drought value map, a potential drought risk management strategy was explored using data collected through the FGD with the stakeholders. To achieve this, the Living Labs methodology was adopted (Atteslander, 2003). This approach is crucial for analyzing stakeholders' perspectives on drought risk reduction through NbS, employing comprehensive participatory procedures and extensive collaborative planning strategies.

NbS for drought management were examined using key informant (KI) interviews, FGD, and field observations focused on pastoralists' variability and coping mechanisms. The study area was stratified into high and low draught vulnerable areas. Four districts were selected, representing eight villages - four from each of the high and low drought-vulnerable areas. Key informants were chosen from local residents with extensive knowledge of the history of the study area, firsthand experience with drought occurrence, and familiarity with coping mechanisms. Six individuals from each district participated in the key informants interviews. Additionally, each district conducted three separate FGDs, with eight representatives from each social group (men, women, and youth) in each discussion. The FGDs facilitated idea exchanges and provided deeper insights into NbS adaptation and coping mechanisms. Field observations were conducted to validate the data collected, focusing on residences, farms, grazing areas, and other local settings. Socioeconomic characteristics along with various NbS drought adaptation and coping mechanisms, were compared across the two strata to identify differences and trends.

3. Results and Discussion

3.1 Mapping of the key variables

3.1.1 LULC, slope, aspect and elevation

DEM that captures landscapes and ground surface topography is crucial to address challenges, including the consequences of climate change, disaster response, environmental management, and water security. Using DEM, the study showed that the south part largely consists of a low-elevation zone, whereas the north mainly consists of high elevations (Figure 3a).

Slope is a key indicator of drought risk. Higher topographic areas experience significantly greater water drainage compared to their neighboring lower areas, making droughts less likely in lower-sloping terrain than on steep plains (Ferreira et al., 2020). Descriptive statistics for slope show a mean of 80.11 and standard deviation of 28.11 with slope ranging from 0 to 89.99^0. Figure 3b shows regional variability of slope.

The aspect, or the direction and orientation of the slope, influences the amount of solar radiation received, which impacts the hydrology of the study area. Variations in solar radiation affect parameters such as temperature, humidity, infiltration, runoff, and soil evaporation, which in turn influence drought vulnerability (Jain et al., 2015). The aspect map of the study area (Figure 3c) was categorized based on these factors, with values assigned to each class, into ten classes to reflect vulnerability levels. Vulnerability classifications for various aspect ranges were developed using relevant literature and local expert knowledge (Ekrami et al., 2016).

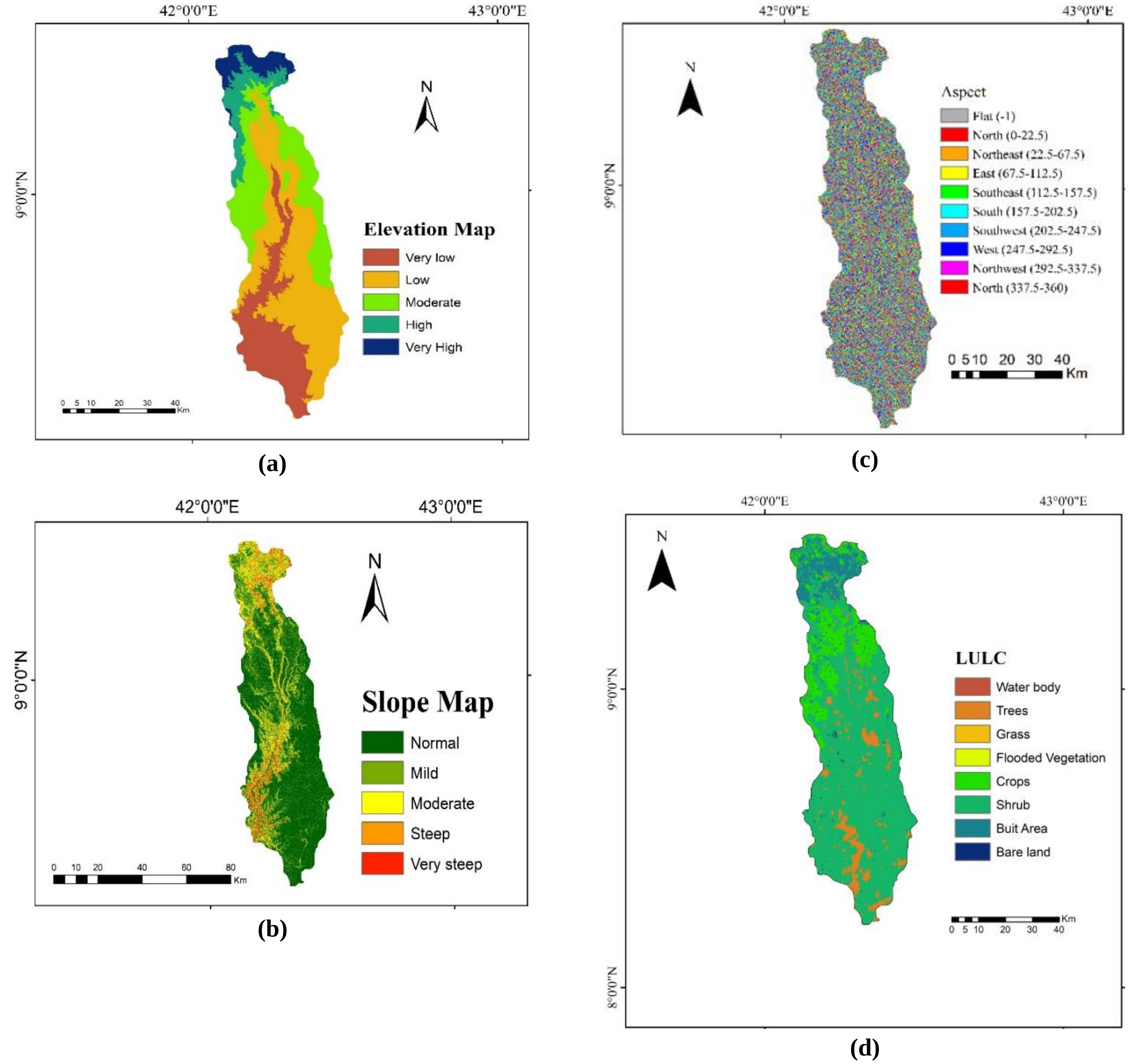

Figure 3: Elevation (a), Slope (b), Aspect (c), and LULC (d)

In addition to topography, societal factors, land use and management practices, and government agricultural practices contribute dynamically to drought susceptibility. Due to its variable nature, land use is recognized as an exposure factor for the study. The dominant land uses in the study area are shrubs (63.74%), crops (18.62%), constructed area (9.45%), grass (4.25%), trees (3.37%), bare land (0.35%), flooded vegetation (0.16%), and water (0.06%). Among the eight identified land-use categories (Figure 3d), agriculture is the most drought-sensitive due to its dependence on water, followed by urban use. Therefore, the agriculture sector received the highest numerical weight value in the drought vulnerability analysis.

3.1.2 Population density, Land Surface Temperature, Normalized Difference Vegetation Index, and Normalized Difference Moisture Index

Population density significantly impacts water usage, making water demand and consumption major challenges in densely populated areas. Regions with higher population densities are consequently more vulnerable to drought than those with lower population densities. This research highlights the critical role of population density, as it directly correlates with increasing water demand and intensifies pressure on water resources as population grow. As population density rises, it exacerbates stress on water sup-ply systems, thereby increasing the likelihood of drought. The Northern part of the sub-basin exhibited a very high population density, resulting in a greater risk of water scarcity and water stress due to rapid population growth (Figure 4a). Higher population density and water stress in this region are strongly associated with socio-economic drought, as dense populations exacerbate resource demands.

To analyze water and energy budgets at the surface-atmosphere interface, Land Surface Temperature (LST), derived from TIR band data, provides critical insights into the state of the terrestrial surface (Bennie et al., 2008). LST (Figure 4b) serves as a key indicator for measuring evapotranspiration, vegetation water stress, soil moisture, and thermal inertia (Gutman, 1990).

Additionally, low values of NDVI indicate stressed plants, particularly in semiarid and arid environments, making NDVI a valuable response variable for detecting and quantifying drought disturbance (Moran et al., 1994). In this study, plant cover was mapped using a Landsat 8 ETM+ image and the NDVI index (Figure 4c). The NDVI, widely used to assess vegetation health, measure photosynthetic activity or “greenness” by converting the red and near-infrared bands images into a vegetation index.

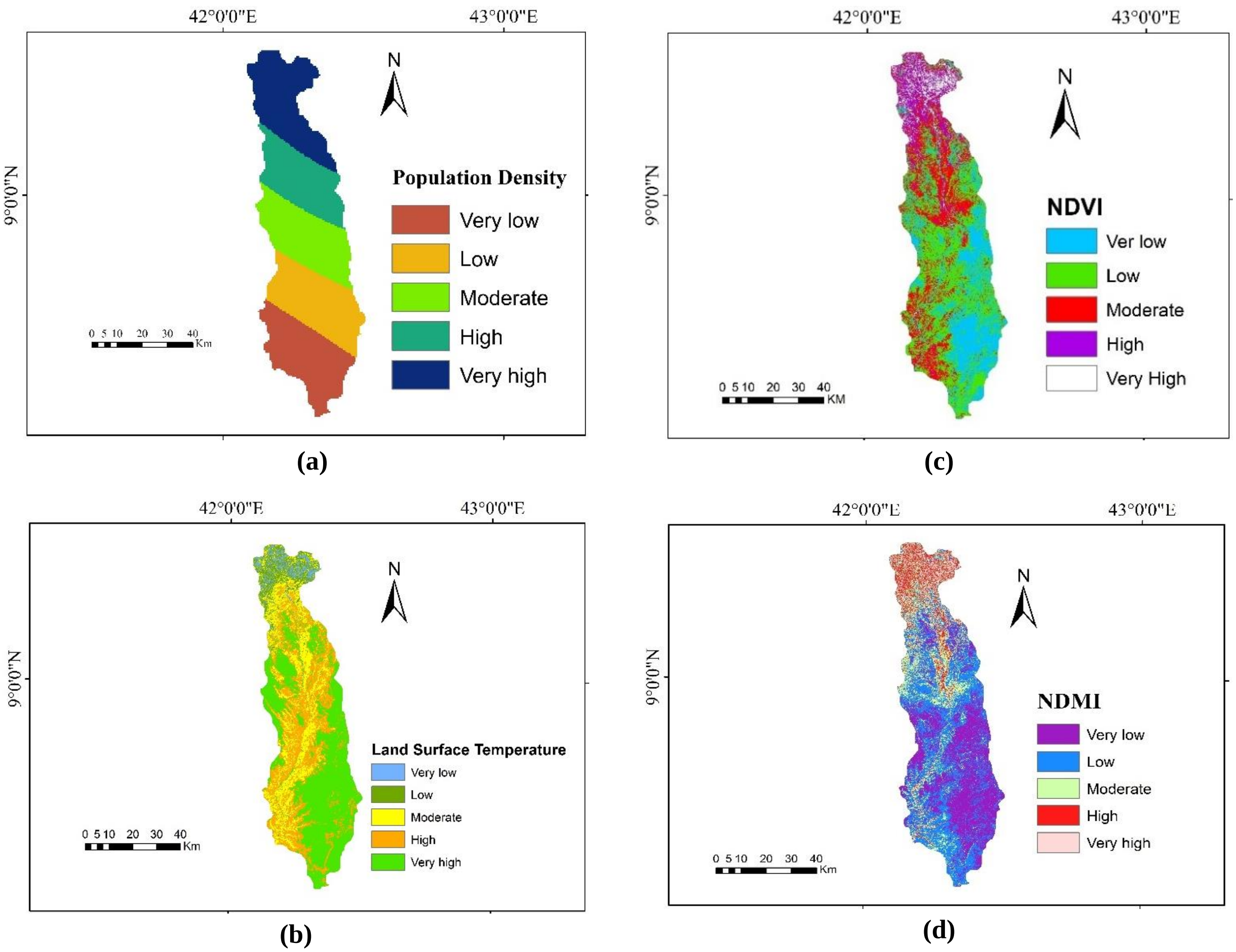

Figure 4: Population density (a), Land Surface Temperature (b), Normalized Difference Vegetation Index, NDVI (c), and Normalized Difference moisture Index, NDMI (d)

The NDVI was calculated using each red and near-infrared wavelength band. The NDVI scale ranges from -1 to +1, with values +1 indicating healthy vegetation (Myneni et al., 1995) and values near -1 indicating saturated water. For this study, only the vegetation cover was considered (Myneni et al., 1995). During drought, vegetative canopies often experience water stress, significantly affecting plant growth, particularly in agricultural areas. The stress can lead to crop failures or reduced yields. However, early diagnosis of plant water stress using NDVI can help mitigate these impacts.

The NDMI closely correlate with plant water content (Figure 4d) and thus, serves as an excellent indicator of plant water stress. Studies have confirmed its effectiveness for drought monitoring and early warning (Tucker & Choudhury, 1987). NDMI is sensitive to changes in liquid water content and the spongy mesophyll in plant canopies, as it is calculated using near-infrared (NIR) and shortwave infrared (SWIR) reflectance (UNDRR, 2021). This makes it a valuable tool for identifying and addressing drought impacts on vegetation.

3.1.3 Vegetation condition index, vegetation health index and soil moisture index

VCI measures variations in the red and near-infrared bands reflected in the spongy mesophyll of the vegetative canopy, driven by chlorophyll absorption and reflection. VCI outperformed other indices, such as NDVI or NDMI alone, in detecting drought conditions across Spain's diverse vegetation (Gu et al. (2008). VCI was developed by Kogan (1997) and scales the NDVI between its minimum and maximum values for each pixel over a significant temporal record beginning in 1981. The current NDVI value is compared with the range of historical NDVI values recorded during the same period in prior years. The VCI is expressed as a percentages where the observed value falls within the historical extremes, with lower values signifying poor vegetation conditions and higher values indicating good conditions. The composite time can represent periods such as a decade, a growth season, a week, a month, or an entire year, with an average NDVI of zero. By normalizing the NDVI, the VCI reduces the influence of spatial and temporal variability in phenology across different land cover types and climates, while emphasizing relative changes in local NDVI signals over time. This metric is widely used to monitor drought and assess vegetation conditions (Figure 5a).

On the other hand, VHI measures drought severity by combining the VCI and TCI. VHI reflects the impact of vegetation health and temperature on plant conditions. The TCI is calculated by comparing current temperature to long-term maximum and minimum temperatures, based on the premise that higher temperatures often worsen vegetative conditions. A lower VHI indicates poor vegetation health and increased stress from high temperatures, which collectively point to dryness over a prolonged period (Figure. 5b). Additionally, the SMI is used to evaluate the soil moisture status, serving as an excellent indicator of drought during dry conditions (Figure 5c).

3.2 Draught vulnerability map

The study found that 30.05% of Erer Sub-basin's land area falls into the intermediate drought class, while the other categories are distributed as extreme drought (19.1%), almost no drought (20%), low drought vulnerability (16.50%), and extremely severe drought (13.60%) (Figure 6). Areas with very high and high drought vulnerability are predominantly located in the Fik and Midhagatola districts. High to very high drought sensitivity was observed in regions characterized by steep slopes, moderate elevation, high to very high NDVI, and moderate to high land surface temperature. These areas have moderate population densities and a significant presence of built-up zones. Similar findings were reported globally (Palchaudhuri and Biswas, 2016; Gao, 1996). Beyond the risk of drought, the lower sub-basin area faces additional significant challenges, including soil dryness, declining groundwater tables, soil erosion, water shortages, deforestation, environmental imbalances, and agricultural failure.

Eerer sub-basin is situated at the confluence of the Wabe Shebelle river plain and its basin, a location shaped by unique lithological conditions that contribute to persistent challenges. The lower sub-basin area spans the Midhagatola, Babile, Fadis and Fik districts (Figure 6), regions characterized by arid climate and acute water scarcity. This area's undulating hard rock terrain is covered by lateritic soil, which has poor water-holding capacity and low fertility. These unfavorable physical conditions severely hinder agricultural productivity and other activities, leaving the population perpetually vulnerable to agricultural and hydrological drought. During the rainy season, the gully erosion exacerbates these challenges as loose debris accumulates in the riverbeds, causing significant flooding and economic loss in the lower basin.

3.3 Stakeholder perceptions and NbS

Eerer sub-basin experiences both drought and flooding annually, a pattern confirmed during FGD with stakeholders. In an attempt to mitigate these issues, the government introduced water harvesting structures across Midhagatola, Babile, Fadis, and Fik districts. The structures were designed to store water during the rainy season and channeled for domestic and agricultural usage in the dry season. Additionally, they aimed to reduce downstream flooding by capturing excess water of wet season. However, these interventions have not successfully mitigated the hydro-meteorological hazards. The affected districts continue to face significant environmental and financial risk. Despite numerous strategies, and concepts applied over the years, the challenges remain unresolved. Adopting NbS offers the most sustainable approach to address these persistent issues by leveraging natural ecosystems to enhance the region's resilience and adaptive capacity.

The crop production system in the study area is highly sensitive to impact of climate change (Renza et al., 2010; Ghosh et al., 2020). Consequently, an increasing number of households are expected to face food insecurity in the future. Climate change poses a significant threat to Ethiopia's crop productivity, as rising growing season temperatures and the high variable rainfall exacerbate drought conditions soil degradation, and declining soil fertility (Lemma & Wondimagegn, 2014; Shukla et al., 2021). These challenges underscore the importance of implementing NbS to protect the agricultural sector.

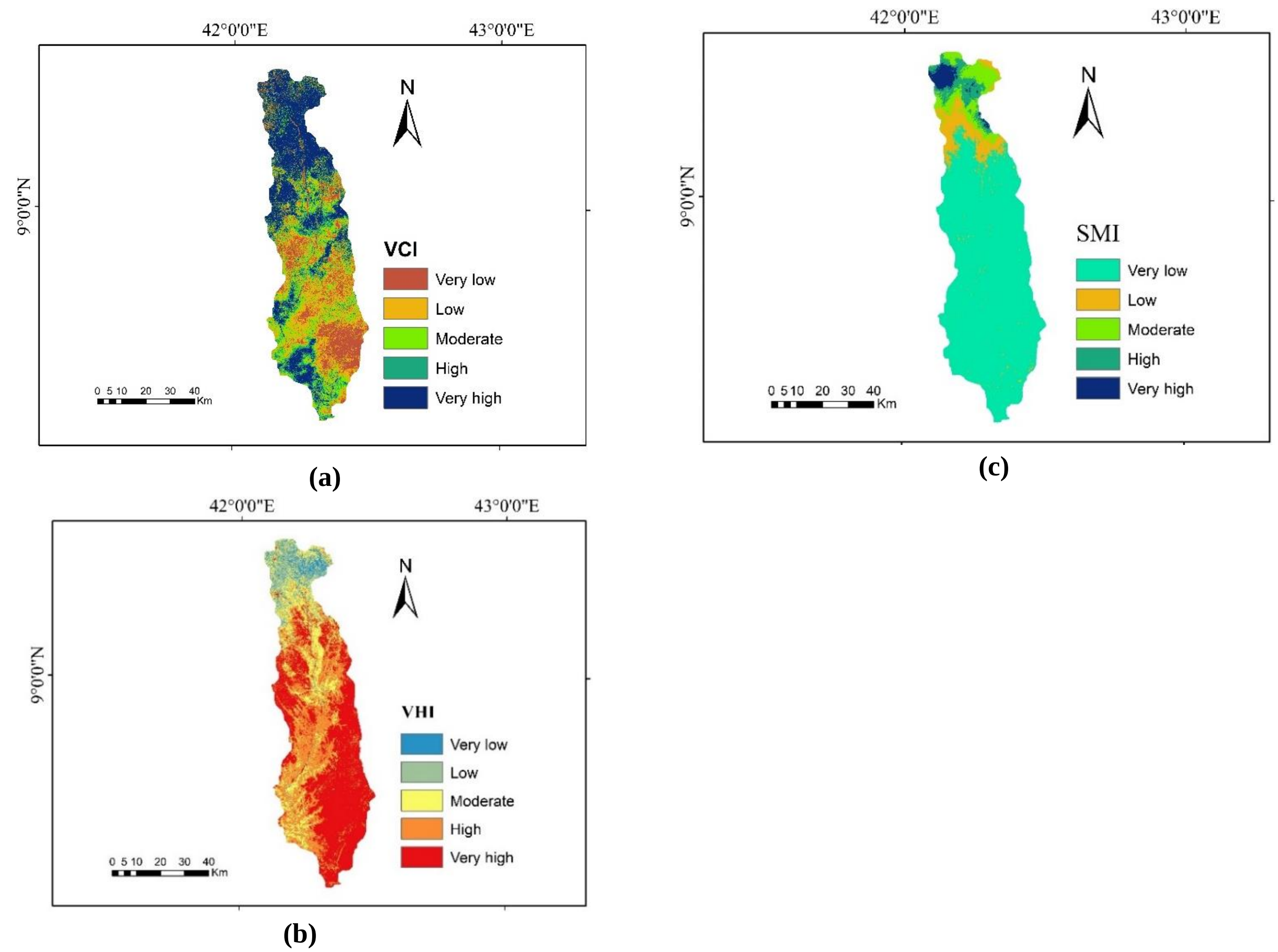

Figure 5: Vegetation Condition Index (a), Vegetation Health Index (b), and Soil Moisture Index (c)

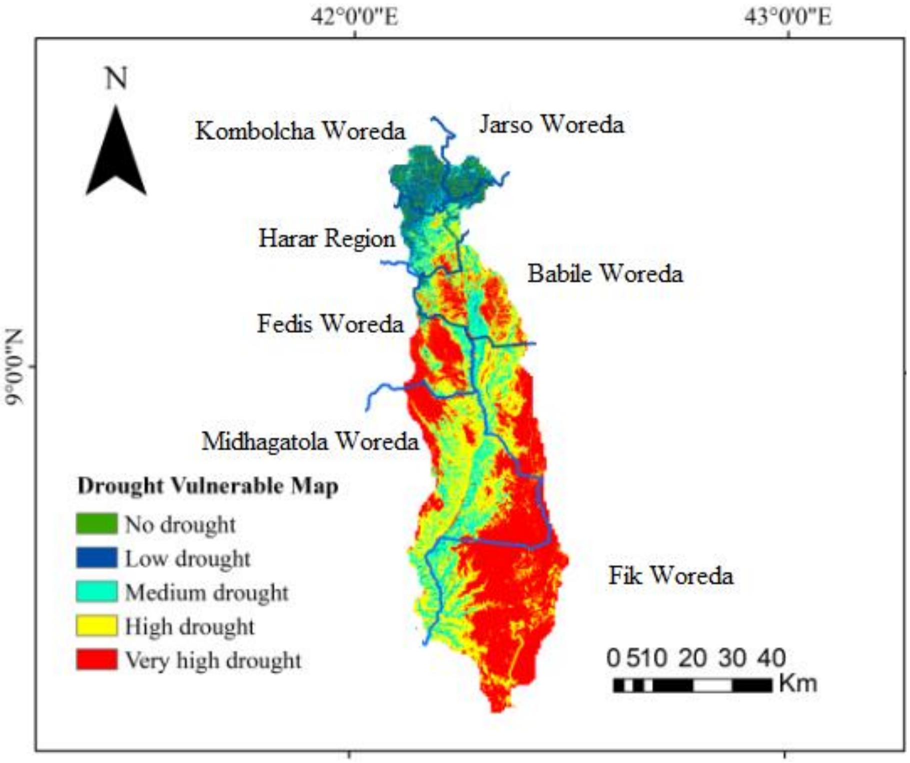

Figure 6: The study area's spatial distribution of drought ('Woreda' is local word for district)

NbS provides sustainable ecological approaches to environmental challenges. In Ethiopia's crop production system, NbS strategies focus on regulating temperature, maintaining soil moisture, and enhancing nitrogen levels as climate change adaptation measures. Ethiopian smallholder farmers have adopted NbS strategies to mitigate drought in vulnerable areas (Tamiru & Fekadu, 2019; Abrham et al., 2017; Tekeste, 2021). These practices include improved crop varieties, use of inorganic fertilizers, conservation agriculture, soil and water management (for example., in-situ water harvesting and soil conservation techniques), agroforestry, adjusted planting dates, organic fertilizers, supplementary irrigation and farmer-led forest landscape regeneration (Abrham et al., 2017; Hana & Edom, 2022; Fiker et al., 2021; Hou Jones et al., 2021).

NbS strategies for drought mitigation, such as farmyard agroforestry, soil and water conservation, and organic fertilizers, help sustainably increase crop productivity by preserving soil moisture and enhancing essential soil nutrients. Additionally, water harvesting has been identified as one of the most crucial methods of addressing water shortages in drought-prone regions (Renza et al., 2010). In East Hararghe, Ethiopia, smallholder farmers who apply climate change adaptation measures, such as altering sowing dates and conserving water, experience better food secure compared to those who do not.

The FGD with smallholder farmers confirmed the widespread use of nature-based practices, including soil and water conservation, farmer-level water harvesting, and drought resistant crop varieties. These practices align with the analysis of drought vulnerability in the sub-basin, which indicates medium to high drought levels. Farmers noted that implementing NbS will help alleviate the impacts of drought, contributing to more sustainable crop production and enhanced resilience in the region.

4. Conclusions

This study characterized drought vulnerable area Eerer Sub-basin, and then proposed long-term nature-based solution. AHP was employed to assess the region, integrating multi-parameter analysis with site-specific variables. The findings revealed that the sub-basin is highly susceptible to drought, with risk factors including low vegetation cover, high population density, steep slopes, and intermediate elevations. The middle sub-basin faces severe flooding during the rainy season, while the downstream area remains at significant drought risk, resulting in substantial economic losses. A long-term strategy is essential to protect the sub-basin by enhancing adaptive capability through carefully selected NbS. These solutions, combined with blue infrastructure for drought risk reduction, offer effective and robust tool for building climate resilience and addressing future risk in the region.

Successful drought risk reduction hinges on understanding ecological changes driven by climate change, rising population, and changing land use patterns. To mitigate the likelihood of hydrological disasters in the sub-basin, the study advocates for stringent regulatory measures and the integration of NbS in densely populated areas. Additionally, leveraging seasonal floods for artificial recharge can help reduce the impact of drought and manage surface runoff. This research provides a foundation for identifying artificial recharge sites and developing strategies that enhance the economic and climatic resilience of the Eerer Sub-basin.

Based on the analysis of this research, the following recommendations are drawn to address drought vulnerability and to enhance resilience in Eerer Sub-basin.(1) Reforestation and vegetation cover improvement educe soil erosion, enhance water retention, and stabilize steep slopes; (2) soil and water conservation measures, such as terracing, contour farming, and mulching, shall reduce water runoff, improve soil moisture, and promote groundwater recharge; (3) artificial recharge structures leverage seasonal floods for artificial groundwater recharge; (4) rainwater harvesting systems, especially in densely populated areas, shall reduce dependence on natural water sources and increase water availability during droughts; (5) public awareness and community participation in conservation and NbS initiatives, promote education on sustainable water management and the use of local knowledge. While the study utilized high-resolution datasets and indicators applicable to other regions, it emphasizes that vulnerability assessments must also consider the socioeconomic and cultural dimensions of affected com-munities for comprehensive risk analysis.

Acknowledgments: The Authors are grateful to the Norwegian Agency for Development Cooperation (NORAD) for the financial support through the Environmental Risk Management under Increasing Extremes and Uncertainty (MERIT) project through Haramaya University. We appreciate the logistic support by Haramaya University. We are also indebted to all MERIT project team members who collaborated with us during project development.

Reference

Abrha Brhan Gebre (2016). Potential effects of agroforestry practices on climate change mitigation and adaptation strategies: a review. *J. Nat. Sci. Res* , 6(15), 83-89.

Abrham Belay, Recha, J. W., Teshale Woldeamanuel, & Morton, J. F. (2017). Smallholder farmers' adaptation to climate change and determinants of their adaptation decisions in the Central Rift Valley of Ethiopia. *Agric & Food Secur, 6, 24.*

Ahamed, T., Rao, K., &, Murthy, J. (2000). GIS-based fuzzy membership model for crop-land suitability analysis. *Agric Syst*, 63(2), 75–95.

Alharbi, R.S., Nath, S., Faizan, O.M., Ul Hasan, M.S., Alam, S.S., Khan, M.A., Bakshi, S., Sahana, M., &, Saif, M.M. (2022). Assessment of Drought vulnerability through an integrated approach using AHP and Geoinformatics in the Kangsabati River Basin. *J. King Saud Univ. Sci.*, 34(8), 102332.

Al-Shabeeb, A.R., Al-Adamat, R. &, Mashagbah, A. (2016). AHP with GIS for a Preliminary Site Selection of Wind Turbines in the North West of Jordan. *Int. J. Geosci.*, 7(10), 1208–1221.

Alsumaiei, A., & Alrashidi, M. (2020). Hydro-meteorological drought forecasting in hyper-arid climates using nonlinear autoregressive neural networks. *Water*, 12(9), 2611.

Artis, D., & Carnahan, W. (1982). Survey of Emissivity Variability in Thermography of Urban Areas. *Remote Sens. Environ*, 12(4), 313–329.

Atteslander, P. (2003). Methoden der empirischen Sozialforschung. Berlin, New York: De Gruyter.

Azhdari, Z., Bazrafshan, O., Zamani, H., Shekari, M., & Singh, V. (2021). Hydro-meteorological drought risk assessment using linear and nonlinear multivariate methods. *Phys. Chem. Earth, Parts A/B/C*, 123, 103046.

Baik, J., Zohaib, M., Kim, U., Aadil, M., & Choi, M. (2019). Agricultural drought assessment based on multiple soil moisture products. *J. Arid Environ*, 167, 43–55.

Bennie, J., Huntley, B., Wiltshire, A., Hill, M., & Baxter, R. (2008). Slope, aspect, and climate: spatially explicit and implicit models of topographic microclimate in chalk grassland. *Ecol. Model*, 216(1), 47–59.

Chander, G., Markham, B., & Helder, D. (2009). Summary of Current Radiometric Calibration Coefficients for Landsat MSS, TM, ETM+, and EO-1 ALI Sensors. *Rem. Sens. Environ*. , 113(5), 893–903.

Chen, Y., Yeh, C., & Yu, B. (2011). Integrated application of the analytic hierarchy process and the geographic information system for flood risk assessment and flood plain management in Taiwan. *Nat Hazards*, 59, 1261–1276.

CSA (2013). Population projection of Ethiopia for all regions at Wereda level from 2014–2017. Addis Ababa: Federal Democratic Republic of Ethiopia.

Dejene W. Sintayehu, Asfaw Kebede Kassa, Negash Tessema, Bekele Girma, Sintayehu Alemayehu , & Jemal Yousuf Hassen (2023). Drought Characterization and Potential of Nature-Based Solutions for Drought Risk Mitigation in Eastern Ethiopia. S*ustainability*, 15(15), 11613.

Demir, G., Aytekin, M., Akgun, A., Ikizler, S., & Tatar, O. (2013). A comparison of landslide susceptibility mapping of the eastern part of the North Anatolian Fault Zone (Turkey) by likelihood-frequency ratio and analytic hierarchy process methods. *Nat Hazards*, 65, 1481–1506.

Demisachew Yilma Gashaw, Karuturi, V., Dessie Nedaw, & Sridhar, G. (2022). Rainwater Harvesting in Modjo Watershed, Upper Awash River Basin, Ethiopia through Remote Sensing and Fuzzy AHP. *Geocarto International*, . 37, 14785–14810.

Deo, R., Byun, H.-R., Adamowski, J., & Begum, K. (2017). Application of effective drought index for quantification of meteorological drought events: A case study in Australia. *Theor. Appl. Climatol*, 128, 359–379.

Ekrami, M., Marj, A., Barkhordari, J., & Dashtakian, K. (2016). Drought vulnerability mapping using AHP method in arid and semiarid areas: a case study for Taft Township, Yazd Province, Iran. Environ. *Earth Sci*., 75, 1039.

Feizizadeh, B., & Blaschke, T. (2013). GIS-multicriteria decision analysis for landslide susceptibility mapping: comparing three methods for the Urmia lake basin, Iran. *Nat Hazards*, 65, 2105–2128.

Ferreira, V., Barreira, A., Loures, L., Antunes, D., & Panagopoulos, T. (2020). Stakeholders' Engagement on Nature-Based Solutions: A Systematic Literature Review. *Sustainability* , 12(2), 640.

Fiker Hilemelekot, Desalegn Yayeh Ayal, Kassahun Ture, & Tadesse Terefe Zeleke (2021). Climate change and variability adaptation strategies and their implications for household food Security : The case of Basona Worena District, North Shewa zone, Ethiopia. *Climate Services*, 100, 100269.

Gao, B. (1996). NDWI A normalized difference water index for remote sensing of vegetation liquid water from space. *Remote Sens. Environ*., 58(3), 257–266.

Ghosh, D., Mandal, M., Banerjee, M., & Karmakar, M. (2020). Impact of hydro-geological environment on availability of groundwater using analytical hierarchy process (AHP) and geospatial techniques: A study from the upper Kangsabati river basin. *Groundwater Sustainable Dev*., 11, 100419.

Gu, Y., Hunt, E., Wardlow, B., Basara, J., Brown, J., & Verdin, J. (2008). Evaluation of MODIS NDVI and NDWI for vegetation drought monitoring using Oklahoma Mesonet soil moisture data. *Geophys. Res. Lett*., 35(22), 1-5.

Gutman, G.G. (1990). Towards Monitoring Droughts from Space. *J. Clim.*, 3, 282– 295.

Hana Tamrat Gebirehiwot, & Edom Kibkab (2022). Nature Based Climate Change Adaptation Measures for Sustainable Crops Production in Ethiopia. *Review. Arch Crop Sci*, 5(1), 141-150.

Hasekiogullari, G., & Ercanoglu, M. (2012). A new approach to use AHP in landslide susceptibility mapping: a case study at Yenice (Karabuk, NW Turkey). *Nat Hazards*, 63, 1157–1179.

Hou Jones, X., Roe, D., & Holland, E. (2021). Nature-based solutions in action: lessons from the frontlin. CAN. Retrieved from https://www.iied.org/20451g.

Hunziker, M. (2000). Einstellung der Bevölkerung zu möglichen Land schaftsentwicklungen in den Alpen. Birmensdorf (CH). Eidgenossische Forschungsanstalt WSL, 157.

IPCC. (2021). Climate Change 2021; The Physical Science Basis. Working Group I Contribution to the Sixth Assessment Report of the Intergovernmental Panel on Climate Change. Cambridge: Cambridge University Press.

Jackson, T., Chen, D., Cosh, M., Li, F., Anderson, M., Walthall, C., & Hunt, E. (2004). Vegetation water content mapping using Landsat data derived normalized difference water index for corn and soybeans. *Remote Sens. Environ*., 92(4), 475–482.

Jain, V., Pandey, R., & Jain, M. (2015). Spatio-temporal assessment of vulnerability to drought. *Nat. Hazards*, 76, 443–469.

Khan, M., Muhammad, N., & El-Shafie, A. (2018). Wavelet-ANN versus ANN-based model for hydro-meteorological drought forecasting. *Water*, 10(8), 998.

Khatiwada, K., & Pandey, V.P. (2019). Characterization of hydro-meteorological drought in Nepal Himalaya: A case of Karnali River Basin. *Weather Clim. Extremes* , 26, 100239.

Khoi, D., Sam, T., Loi, P., Hung, B., & Nguyen, V. (2021). Impact of climate change on hydro-meteorological drought over the Be River Basin, Vietnam. *J. Water Climate Change*, 12(7), 3159–3169.

Kogan, F.N. (1997). Global drought watch from space. Bull. Am. *Meteorol. Soc.* , 78(4), 621–636.

Lange, B., Holman, I., & Bloomfield, J.P. (2017). A framework for a joint hydro-meteorological-social analysis of drought. *Sci. Total Environ*. , 578, 297–306.

Lemma Zemedu & Wondimagegn Mesfin (2014). Smallholder's Vulnerability to Food Insecurity and Coping Strategies: In the Face of climate change, East Hararghe, Ethiopia. *J Econ Sustain Dev*, 5(24), 86-100.

Ma, M., Ren, L., Yuan, F., Jiang, S., Liu, Y., Kong, H., & Gong, L. (2014). A new standardized Palmer drought index for hydro-meteorological use. *Hydrol. Process*. , 28(23), 5645–5661.

Malczewski, J. (2006). GIS-based multicriteria decision analysis: a survey of the literature. *Int J Geogr Inf Sci*, 20(7), 703–726.

Marshall, C., & Rossman, G. B. (1998). Designing Qualitative Research. Sage, 321.

Mayring, P. (2010). Handbuch Qualitative Forschung in der Psychologie. In G. M. Mey, Qualitative Inhaltsanalyse. VS Verlag für Sozialwissenschaften/Springer Fachmedien Wiesbaden GmbH.

Miralles, D., Gentine, P., Seneviratne, S., & Teuling, A. (2019). Land–atmospheric feedbacks during droughts and heatwaves: state of the science and current challenges. Ann. N. Y. *Acad. Sci*., 1436(1), 19–35.

Mitchard, E.T.A. (2018). The tropical forest carbon cycle and climate change. *Nature*, 559, 527–534.

MOA (2000). Agro-ecological Zones of Ethiopia. Minstry of Agriculture, Addis Ababa, Ethiopia.

Moran, M., Clarke, T., Inoue, Y., & Vidal, A. (1994). Estimating crop water deficit using the relation between surface-air temperature and spectral vegetation index. *Remote Sens. Environ*., 49(3), 246–263.

Murray-Webster, R., & Simon, P. (2006). Making Sense of Stakeholder Mapping. PM World Today, VIII,(11).

Myneni, R., Hall, F., Sellers, P., & Marshak, A. (1995). The interpretation of spectral vegetation indexes. IEEE Trans. Geosci. *Remote Sens* , 33(2), 481–486.

Palchaudhuri, M., & Biswas, S. (2016). Application of AHP with GIS in drought risk assessment for Puruliya district. India. *Nat Hazards*, 84, 1905–1920.

Prakash, P., Garg, P., & Ghosh, S. (2006). GIS-based modeling for drought assessment. 26th Annual ESRI international user conference, August 7–11, San Diego, California.

Rahmati, O., Falah, F., Dayal, K.S., Deo, R.C., Mohammadi, F., Biggs, T., Moghaddam, D.D., Naghibi, S.A., & Bui, D.T. (2020). Machine learning approaches for spatial modeling of agricultural droughts in the south-east region of Queensland Australia. *Sci. Total Environ*, 699, 134230.

Rather, R.A., Bano, H., Padder, S.A., Perveen, K., Al Masoudi, L.M., Alam, S.S., Hong, S.H. (2022). Anthropogenic impacts on phytosociological features and soil microbial health of Colchicum luteum L. an endangered medicinal plant of North Western Himalaya. *Saudi J. Biol. Sci*., 29(4), 2856–2866.

Reed, M. S., Graves, A., Dandy, N., Posthumus, H., Hubacek, K., & Morris, J., Prell, C., Quinn, C.H., & Stringer, L.C. (2009). Who's in and Why? A Typology of Stakeholder Analysis Methods for Natural Resource Management. *J. Environ. Manag*., 90(5), 1933–1949.

Rehana, S., & Naidu, G. (2021). Development of hydro-meteorological drought index under climate change–Semi-arid river basin of Peninsular India. *J. Hydrol*, 594, 125973.

Rehman, S., Hasan, M. S., Rai, A. K., Rahaman, M. H., Avtar, R., & Sajjad, H. (2022). Integrated approach for spatial flood susceptibility assessment in Bhagirathi sub-basin, India using entropy information theory and geospatial technology. *Risk Analysis*, 42(12), 2765–2780.

Renza, D., Martinez, E., Arquero, A., & Sanchez, J. (2010). Drought estimation maps by means of multidate Landsat fused images. 30th EARSeL Symposium (pp. 775-782). Proceedings of the 30th EARSeL Symposium.

Saaty, T. (2008). Decision-making with the analytic hierarchy process. *Int J Serv Sci* , 1(1), 83–98.

Shukla, R., Gleixner, S., Amsalu Woldie Yalew, Schauberger, B., Sietz, D., & Gornott, C. (2021). Dynamic vulnerability of smallholder agricultural systems in the face of climate change for Ethiopia. *Environ Res Lett*, 16(4), 044007.

Sivakumar, V.L., Krishnappa, R.R., & Nallanathel, M. (2021). Drought vulnerability assessment and mapping using multi-Criteria decision making (MCDM) and application of Analytic Hierarchy Process (AHP) for Namakkal District, Tamilnadu, India. *Mater. Today: Proc*., 43(2), 1592–1599.

Stefanidis, S., & Stathis, D. (2013). Assessment of flood hazard based on natural and anthropogenic factors using analytic hierarchy process (AHP). *Nat Hazards*, 68, 569–585.

Strauss, A., & Corbin, J. M. (1990). Basics of qualitative research: Grounded theory procedures and techniques. Sage Publications, Inc.

Strout, J. M., Oen, A. M., Kalsnes, B. G., Solheim, A., Lupp, G., Pugliese, F., & Bernardie, S. (2021). Innovation in NBS Co-design and Implementation. *Sustainability* , 13(2), 986.

Sur, C., Park, S., Kim, T., & Lee, J. (2019). Remote sensing-based agricultural drought monitoring using hydro-meteorological variables. *KSCE J. Civ. Eng.* , 23, 5244–5256.

Tadesse Zeleke, Giorgi., F., Gulilat Tefera Diro, & Zaitchik., B. F. (2017). Trend and periodicity of drought over Ethiopia. *Int J Climatol* , 37(13).

Tamiru Lemi & Fekadu Hailu. (2019). Effects of climate change variability on agricultural productivity. *Int J Environ Sci Nat Res.*, 17(1), 555953.

Tekeste Kifle. (2021). Climate-Smart Agricultural (CSA) practices and their implications to food security in Siyadebrina Wayu District, Ethiopia. *Afr J Agric Res*, 17(1):92-103.

Tucker, C., & Choudhury, B. (1987). Satellite remote sensing of drought conditions. *Remote Sens. Environ*, 23(2), 243–251.

Ul Hasan, M.S., & Rai, A.K. (2020). Groundwater quality assessment in the Lower Ganga Basin using entropy information theory and GIS. *J. Clean. Prod.* , 274, 123077.

UNDRR. (2021). GAR Special Report on Drought . Geneva: United Nations Office for Disaster Risk Reduction .

Valor, E., & Caselles, V. (1996). Mapping Land Surface Emissivity from NDVI: Application to European, African and South American Areas. *Remote Sens. Environ* , 57(3), 167–184.

Vu, M.T., Vo, N.D., Gourbesville, P., Raghavan, S.V., & Liong, S-Y.. (2017). Hydro-meteorological drought assessment under climate change impact over the Vu Gia-Thu Bon River basin, Vietnam. *Hydrol. Sci. J.*, 62, 1654–1668.

Ying, X., Guang-Ming, Z., Gui-Qiu, C., Lin, T., Ke-Lin, W., & Dao-You, H. (2007). Combining AHP with GIS in the synthetic evaluation of eco-environment quality a case study of Hunan Province. China. *Ecol Model*, 209, 97–109.

Zingraff-Hamed, A., Hüesker, F., Lupp, G., Begg, C., Huang, J., Oen, A., Vojinovic, Z., Kuhlicke, C. & Pauleit, S. (2020). Stakeholder Mapping to Co-create Nature-Based Solutions: Who Is on Board? *Sustainability*, 12(20), 8625.